euspen's 20th International Conference & Exhibition, Geneva, CH, June 2020
www.euspen.eu

Measurement error model for laser line scanners

M. Vlaeyen[1], B. Boeckmans[1], H. Haitjema[1], W. Dewulf[1]

[1]*KU Leuven, Department of Mechanical Engineering, Celestijnenlaan 300, B-3001 Leuven, Belgium*

michiel.vlaeyen@kuleuven.be

Abstract
This paper presents an unambiguous method to obtain the measurement error model of a laser line scanner, comprising both the systematic error and the random error of a measurement with this type of optical probing system. A ring gauge is used as artefact for the acquisition of the data required for determining the measurement error model. The model expresses the systematic and random error as a function of the measurement track settings. The considered settings are the distance, the in-plane angle and the out-of-plane angle of the laser line scanner relative to the measurand's surface. The model enables the compensation of systematic errors after calibration in order to improve the accuracy of the measuring system. Furthermore it allows to simulate the propagation of errors on a measurement in order to determine the task-specific measurement uncertainty using a Monte Carlo method. The validation of the measurement error model consists of the evaluation of multiple compensated measurements on ring gauges with varying diameters and similar surface properties as the acquisition artefact.

Keywords: Coordinate measuring machine (CMM), Metrology, Measurement, Uncertainty

1. Introduction

The ongoing trend in the manufacturing metrology requires measurement systems that can achieve 100% quality assurance. Due to measurement uncertainty, conformity to the imposed specifications can however not be warranted for measurement results close to the tolerance limits. If the measurement uncertainty is unknown, it is impossible to prove conformance according to ISO 14253-1 [1]. This is why the Guide to the Expression of Uncertainty in Measurement (GUM) [2,3] requires every measurement result to be accompanied by a measurement uncertainty. The complete quality inspection of all products is unrealistic with conventional and time consuming contact measurement methods. Optical probes, such as laser line scanners (LLSs), form an appealing alternative for tactile probes, because of their non-contact character, the high measuring speed of up to 70 000 points per second and the creation of high density point clouds [4,5]. Despite the considerable improved accuracy over the last decades, the LLS still lacks accuracy compared to tactile measurements [6,7]. Today no robust method exists to determine the uncertainty model of a LLS, which is obviously problematic for a measurement device. The ISO 15530 standard discusses the accuracy verification of contact and non-contact probing systems used on a coordinate measurement machine (CMM), but does not describe a protocol to obtain an uncertainty model. Despite ample research, investigating the effect of individual influence factors on the LLS accuracy, an encompassing task-specific uncertainty determination solution has not yet been developed [8-13]. Therefore to overcome this lack in standardization this paper introduces a method to obtain the measurement error model for a LLS in function of the measurement track settings. The role for this error model is twofold. On the one hand the model expresses a systematic error, which can be compensated in order to improve the accuracy. On the other hand the measurement uncertainty model expresses the random error. It can be used to express the task-specific measurement uncertainty according to ISO GUM [2,14] or to prove conformance according to ISO 14253-1 [1]. This paper provides the experimental results for the validation of the measurement error model.

2. Error components of a laser line scanner

An LLS projects one or more planes of laser light onto the measurand's surface and tracks the intersection with the object's surface with a camera, thus allowing the determination of surface coordinates by triangulation. The LLS's performance is dependent on multiple parameters, including surface properties (material, surface roughness, color, reflection, etc.) as well as measurement track settings: the distance between the inspected surface and the laser source, also referred to as scan depth, the in-plane angle and out-of-plane angle between the laser line scanner and the surface (Figure 1) [15-17]. The measurement track settings are controlled by the CMM. The measurement error of laser line scanning data has two direction components: the axial and radial direction. The axial direction is from the scanned point towards the CCD sensor of the LLS. The radial direction is perpendicular to the axial direction and is neglectable compared to the axial error. The axial error consists of a systematic error compared with calibrated data and a random error. Both errors are related to the measurement track settings. The measurement error model for the axial error is set up in function of the measurement track settings, assuming the other error contributors are stable. The model is thus only valid for materials with similar surface properties.

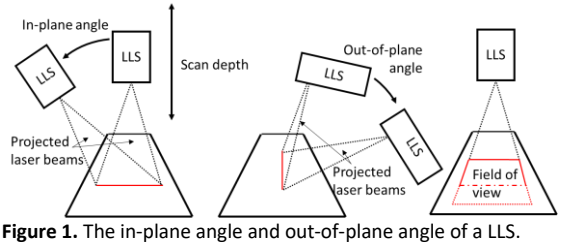

Figure 1. The in-plane angle and out-of-plane angle of a LLS.

3. Obtaining the measurement error model

The proposed method to obtain the model requires an artifact with uniform surface properties, in order to exclude the influence of different error components as those mentioned earlier. The collection of data is unambiguous: points on the artifact are measured with a LLS and a measurement method that is at least one order of magnitude more accurate, i.e. tactile probing, as a reference. Data is collected from multiple scan paths by manipulating the position of the LLS relative to the artefact (Figure 2). In order to maximize the covered surface, the scan trajectory is chosen perpendicular to the field of view. However the orientation of the scanner is kept constant in order to exclude the additional uncertainty due to the CMM articulating probing system. Due to the fixed orientation a curved surface, i.e. a cylinder or a sphere, is preferable to a flat surface in order to maximize the variation of the envisioned parameters: scan depth, in-plane angle and out-of-plane angle. The artefact should also be suitable for tactile measurements. Therefore the chosen artifact is a ring gauge.

Knowing the orientation and path of the LLS and the reference position of the feature, the distance between the scanned point and the LLS, the out-of-plane and in-plane angle and error can be determined for each obtained point. Also the measurement error is calculated locally. A graphical interpretation for the following mathematical calculation is given in Figure 3. Point X_s is a scanned point of the data obtained by a scan from the scan path of the laser source with start, S, and end point, E. The mathematical expression of the scan path is:

$$\overrightarrow{SE} + \begin{Bmatrix} S_x \\ S_y \\ S_z \end{Bmatrix} = 0 \tag{1}$$

A plane Ω can be expressed as set of points Ψ where $\overrightarrow{SE}$ is a normal vector to the plane. Since the scan trajectory is perpendicular to the field of view and X_s is a point on the plane:

$$\left\{ \Psi \middle| \left(\Psi - \begin{Bmatrix} \mathrm{X_{s,x}} \\ \mathrm{X_{s,y}} \\ \mathrm{X_{s,z}} \end{Bmatrix} \right) \cdot \overrightarrow{SE} = 0 \right\} \tag{2}$$

The position of the laser source, X_0, can be found along the scan path, with d a scalar:

$$\begin{Bmatrix} X_{0,x} \\ X_{0,y} \\ X_{0,z} \end{Bmatrix} = d \cdot \overrightarrow{SE} + \begin{Bmatrix} S_x \\ S_y \\ S_z \end{Bmatrix} \tag{3}$$

Since X_0 is the intersection of plane Ω and $\overrightarrow{SE}$, d can be found by substituting equation (3) into equation (2):

$$\left(d\overrightarrow{SE} + \begin{Bmatrix} S_x \\ S_y \\ S_z \end{Bmatrix} - \begin{Bmatrix} \mathrm{X_{s,x}} \\ \mathrm{X_{s,y}} \\ \mathrm{X_{s,z}} \end{Bmatrix} \right) \cdot \overrightarrow{SE} = 0$$

$$\Leftrightarrow d = \frac{\left(\begin{Bmatrix} \mathrm{X_{s,x}} \\ \mathrm{X_{s,y}} \\ \mathrm{X_{s,z}} \end{Bmatrix} - \begin{Bmatrix} S_x \\ S_y \\ S_z \end{Bmatrix} \right) \cdot \overrightarrow{SE}}{\overrightarrow{SE}^2} \tag{4}$$

The orientation of the laser beam, $\vec{v}$, goes from the laser source, X_0, towards the scanned point, X_s. Based on the reference information a cylinder is created with center point, C, and central axis, $\vec{a}$. The calibrated point, X_c, can be found as the intersection of the laser beam and the reference cylinder. The distances between X_0 and X_s and between X_0 and X_c are respectively:

$$d(X_0, X_s) = \sqrt{\left(X_{0,x} - \mathrm{X_{s,x}}\right)^2 + \left(X_{0,y} - \mathrm{X_{s,y}}\right)^2 + \left(X_{0,z} - \mathrm{X_{s,z}}\right)^2} \tag{5}$$

$$d(X_0, X_c) = \sqrt{\left(X_{0,x} - \mathrm{X_{c,x}}\right)^2 + \left(X_{0,y} - \mathrm{X_{c,y}}\right)^2 + \left(X_{0,z} - \mathrm{X_{c,z}}\right)^2} \tag{6}$$

The scan depth is expressed by equation (6) and the measurement error, ε, is the difference between equation (5) and (6):

$$\varepsilon = d(X_0, X_s) - d(X_0, X_c) \tag{7}$$

Notice that calculating the distance between X_s and X_c as a measurement error will result in only positive values, while in reality the measurement error can also be negative.

For the calculation of the remaining track settings, namely the in-plane angle and out-of-plane angle, the normal, $\vec{n}$, on the reference surface in X_c needs to be known. The normal is perpendicular to the axis of the cylinder, therefore:

$$\vec{a} \cdot \vec{n} = 0 \tag{8}$$

Assume that T is the intersection of the normal and the central axis. Then the normal can be written as vector from X_c to T:

$$\vec{n} = T - X_c \tag{9}$$

Since T lies on the central axis, the following equation with t a scalar applies:

$$\begin{Bmatrix} T_x \\ T_y \\ T_z \end{Bmatrix} = t \cdot \vec{a} + \begin{Bmatrix} C_x \\ C_y \\ C_z \end{Bmatrix} \tag{10}$$

Substitution of (9) in (8) gives:

$$\vec{a} \cdot \left(\begin{Bmatrix} T_x \\ T_y \\ T_z \end{Bmatrix} - \begin{Bmatrix} \mathrm{X_{c,x}} \\ \mathrm{X_{c,y}} \\ \mathrm{X_{c,z}} \end{Bmatrix} \right) = 0 \tag{11}$$

and substitution of (10) in (11) gives:

$$\vec{a} \cdot \left(t\vec{a} + \begin{Bmatrix} C_x \\ C_y \\ C_z \end{Bmatrix} - \begin{Bmatrix} \mathrm{X_{c,x}} \\ \mathrm{X_{c,y}} \\ \mathrm{X_{c,z}} \end{Bmatrix} \right) = 0$$

$$\Leftrightarrow t = \frac{\vec{a} \cdot \left(\begin{Bmatrix} \mathrm{X_{c,x}} \\ \mathrm{X_{c,y}} \\ \mathrm{X_{c,z}} \end{Bmatrix} - \begin{Bmatrix} C_x \\ C_y \\ C_z \end{Bmatrix} \right)}{\vec{a}^2} \tag{12}$$

The normal can be found by the substitution of equation (11) and (10) in equation (9):

$$\vec{n} = \frac{\vec{a} \cdot \left(\begin{Bmatrix} \mathrm{X_{c,x}} \\ \mathrm{X_{c,y}} \\ \mathrm{X_{c,z}} \end{Bmatrix} - \begin{Bmatrix} C_x \\ C_y \\ C_z \end{Bmatrix} \right)}{\vec{a}^2} \vec{a} + \begin{Bmatrix} C_x \\ C_y \\ C_z \end{Bmatrix} - \begin{Bmatrix} \mathrm{X_{c,x}} \\ \mathrm{X_{c,y}} \\ \mathrm{X_{c,z}} \end{Bmatrix} \tag{13}$$

The angle between the normal on the surface and the laser beam consists out of two components: the in-plane angle, α_{in}, and out-of-plane angle, α_{out}. To calculate both angles, the normal is split in two vectors: $\overrightarrow{v_{in}}$, the projection of the normal on the field of view and $\overrightarrow{v_{out}}$, the projection on the plane perpendicular to the field of view:

$$\overrightarrow{v_{in}} = \vec{n} - \frac{\vec{n} \cdot \overrightarrow{SE}}{\|\vec{n}\|^2} \overrightarrow{SE} \tag{14}$$

$$\overrightarrow{v_{out}} = \vec{n} - \frac{\vec{n} \cdot (\overrightarrow{SE} \times \vec{v})}{\|\vec{n}\|^2} (\overrightarrow{SE} \times \vec{v}) \tag{15}$$

The in-plane and out-of-plane angle for each point on the surface can be calculated as follows:

$$\alpha_{in} = \begin{cases} if\ \arccos\left(\frac{\overrightarrow{v_{out}} \cdot \overrightarrow{SE}}{\|\overrightarrow{v_{out}}\| \|\overrightarrow{SE}\|} \right) \geq 90°: -\arccos\left(\frac{\overrightarrow{v_{out}} \cdot \overrightarrow{ES}}{\|\overrightarrow{v_{out}}\| \|\overrightarrow{ES}\|} \right) \\ if\ \arccos\left(\frac{\overrightarrow{v_{out}} \cdot (\overrightarrow{SE} \times \vec{v})}{\|\overrightarrow{v_{out}}\| \|\overrightarrow{SE}\|} \right) < 90°: \arccos\left(\frac{\overrightarrow{v_{out}} \cdot \overrightarrow{ES}}{\|\overrightarrow{v_{out}}\| \|\overrightarrow{ES}\|} \right) \end{cases} \tag{16}$$

$$\alpha_{out} = \begin{cases} if\ \arccos\left(\frac{\overrightarrow{v_{in}} \cdot (\overrightarrow{SE} \times \vec{v})}{\|\overrightarrow{v_{in}}\| \|\overrightarrow{SE} \times \vec{v}\|} \right) \geq 90°: -\arccos\left(\frac{\overrightarrow{v_{in}} \cdot \overrightarrow{ES}}{\|\overrightarrow{v_{in}}\| \|\overrightarrow{ES}\|} \right) \\ if\ \arccos\left(\frac{\overrightarrow{v_{in}} \cdot (\overrightarrow{SE} \times \vec{v})}{\|\overrightarrow{v_{in}}\| \|\overrightarrow{SE} \times \vec{v}\|} \right) < 90°: \arccos\left(\frac{\overrightarrow{v_{in}} \cdot \overrightarrow{ES}}{\|\overrightarrow{v_{in}}\| \|\overrightarrow{ES}\|} \right) \end{cases} \tag{17}$$

For all the obtained data these three parameters (scan depth, in-plane angle and out-of-plane angle) accompanied with their corresponding measurement error are calculated. A least-squares best fit, with the scan depth, the in-plane and the out-of-plane angle as independent variables and the measurement error as dependent variable is created to characterize the systematic error. The characterization of the systematic error is based on a second degree polynomial function. The measurement noise is normally distributed, in which case the standard deviation is a good expression for the random error according to ISO GUM. Based on the variation of the data compared to the function of the systematic error, a second degree polynomial function to express the random error is determined. This model includes the uncertainty of the LLS and the Cartesian movement of the CMM.

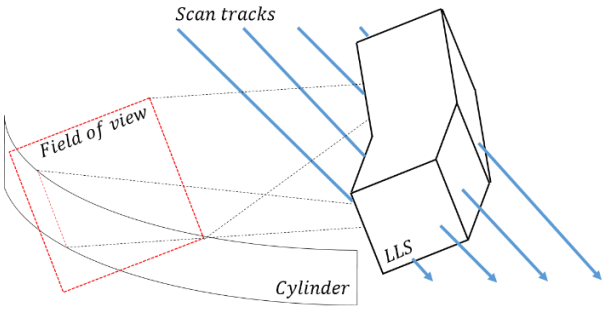

Figure 2. The procedure for the data acquisition for determination of the measurement error model.

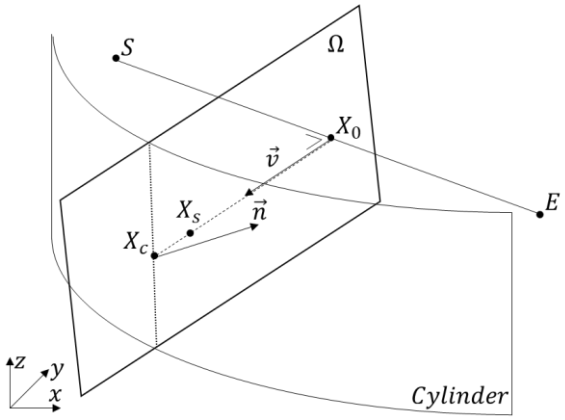

Figure 3. Graphical interpretation for the calculation of the measurement error and the corresponding track settings.

4. Validation of measurement error model

In this section the robustness of the measurement error model is scrutinized. Firstly, the compensation of the measured data is investigated, in order to improve the accuracy of the measured diameter of ring gauges of several diameters. An improvement of the accuracy on the different artifacts with similar surface properties proves the correctness of the systematic error model. Secondly, the measurement uncertainty is determined based on a Monte Carlo method. Simulations obtained with both the systematic error model and the random error model are used in this method. Resemblances between simulations and multiple measurements are an indication of the validity of the model.

Figure 4. Set of ring gauges used for the experiments. The diameters are from left to right 50 mm, 70 mm, 90 mm and 125 mm respectively.

4.1. Evaluation of the systematic error model

In order to validate the compensation of the systematic errors of the laser scanned data, a reference measurement on the ring gauges is performed. The tactile measurement is one order of magnitude more accurate than laser scanning and will serve as a reference for the location and the orientation. Based on the tactile data the position and orientation of the least squares fitted cylinder is determined. The calibrated diameter of the ring gauges is obtained from its specifications. As explained in section 3, the distance between the LLS and the reference surface, the in-plane angle and the out-of-plane angle for each measured point are determined. These three parameters are the input of the polynomial function, which models the systematic error. The scanned data is projected along the direction of the laser beam with the corresponding output of this polynomial function. The outcome is a new point cloud which compensates the systematic error on each point. Then the relevant parameters are determined from the least squares fitting cylinder through the compensated point cloud.

The validation experiment consists of five repeated measurements with the same scan trajectory per ring gauge. There are four ring gauges with a varying diameter of 50 mm, 70 mm, 90 mm and 125 mm. Measurements are performed with a Nikon Metrology LC60Dx LLS mounted on an LK Altera 15.7.6 CMM. For each individual measurement point the systematic error is compensated. The diameter of the least squares fitting cylinder is determined for the original data and for the compensated data. The error on the diameter is the difference in diameter of the measured or compensated data and the reference diameter. The error is caused by the variation of the systematic error: the systematic error increases with an increasing out-of-plane angle. Through this the cylinder segment will appear more curved, which results in a smaller diameter of the least squares fitted cylinder. Figure 5 shows the comparison of the error on the diameters of both the compensated and the original measurement. This result clearly indicates that compensation based on the systematic error model improves the accuracy of the measurement, independent of the diameter of the ring gauge. It has to be mentioned that cylinders are rarely measured from only one side in practice, so in practice errors of this magnitude are rarely met. The 95% confidence interval, expressed by the error bars in Figure 5, are determined by the Monte Carlo simulations, as explained in section 4.2. Fifty simulations are preformed to calculate the measurement uncertainty based on the random error model.

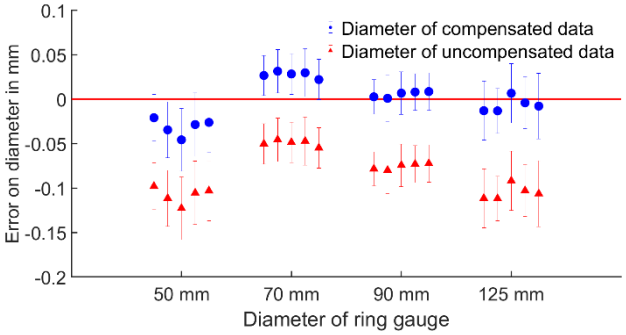

Figure 5. The error and the 95% confidence interval of the diameters of the least squared fitted cylinders.

4.2. Evaluation of the random error model

In order to experimentally determine the measurement uncertainty, fifty repeated measurements are executed with the same scan trajectory on a ring gauge with a diameter of 125 mm. Figure 6 illustrates the variation of the least squares diameter calculated from the original and compensated data. Figure 6 shows that the compensation has no influence on the repeatability of the outcome. These measurements are the reference in the comparison with the diameters of the simulated point clouds. In order to determine the measurement uncertainty the Monte Carlo method is used; virtual measurements are simulated based on the systematic error model and the random error model.

The procedure tracks the following steps. The position of each point on the least squares fitting cylinder of the compensated data is determined during the compensation of the systematic

error. Also the three parameters related to the measurement approach are calculated for each point. This allows to determine the systematic and random error with the measurement error model. Since the simulations are compared to real data, external uncertainty contributors need to be taken into account. These contributors cause deviations in the systematic error model. The deviation is simulated by multiplying the systematic error model with a factor, K. This factor is randomly determined out of a normal distribution. The 95% confidence interval of the fifty repeated measurements is determined and the corresponding variance is 0.01:

$$K \sim \mathcal{N}(1; 0.01) \quad (18)$$

The influence of the external uncertainty contributors on the random error model is marginal in a simulation and is neglected. The position of each point is projected along its opposite view direction with the combined distance of the systematic and random error. The least squares cylinder is fitted on this simulated point cloud. Based on multiple simulations the task specific measurement uncertainty can be determined.

Figure 7 shows the measurement uncertainty determination for one of the fifty reference measurements. Fifty simulations are used to determine the variation of the diameters on both the original data and the compensated data caused by the uncertainty contributors. A comparison between the reference measurements and the simulations shows a similar standard deviation, which confirms the validity of the uncertainty determination method.

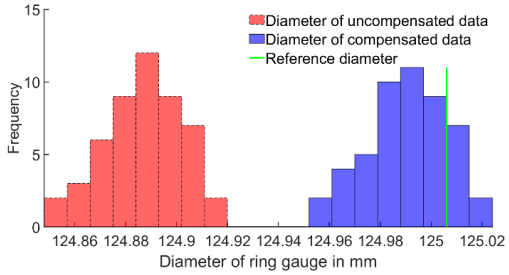

Figure 6. The measurement repeatability of fifty measurements on a ring gauge with diameter of 125 mm before and after the systematic error compensation.

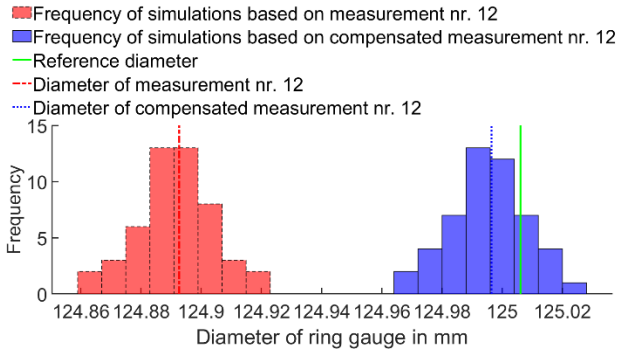

Figure 7. The measurement uncertainty on the diameter of ring gauge with a diameter of 125 mm determined by the Monte Carlo principle based on one of the repeated measurements (before and after compensation).

5. Conclusion

This paper presents a method to obtain a model to express the systematic error and random error of a measurement with a LLS. The mathematical background is given to determine both models based on multiple measurement with different scan trajectories on a calibrated artefact. The used artefact in this paper is a ring gauge, however the method allows any curved artefact for the data acquisition. Based on this model the systematic error of a measurement on varying objects with similar surface properties can be compensated. The systematic error model is validated on four ring gauges with different diameters. The validation shows that the compensation improves the accuracy of the measured diameter of a cylinder. The systematic and random error model allowed to determine the measurement uncertainty on the diameter using the Monte Carlo principle. Within this paper the predicted confidence interval is validated by comparing it with the data of fifty repetitive measurements. Overall these measurement error models allow to improve the accuracy of a state-of-the-art measurement and the models provide an uncertainty budget according to the ISO GUM.

The procedure to compensate the systematic error on laser scanned data relies on a tactile measurement of the radius, orientation and center point of the cylinder. The necessity to fully measure the cylinder tactily makes the laser scanning obsolete. Therefore a method to find the parameters of the cylinder and compensate the systematic error solely based on laser scanned data still needs to be introduced.

References

[1] ISO 14253-1:2011, GPS – Inspection by measurement of workpieces and measuring equipment – Part 2: Guide to the estimation of uncertainty in GPS measurement, in calibration of measuring equipment and in product verification

[2] JCGM 100:2008, Guide to the Expression of Uncertainty in Measurement (GUM): Evaluation of measurement data – Guide to the expression of uncertainty in measurement

[3] Haitjema H. 2011 Task specific uncertainty estimation in dimensional metrology *Int. J. Prec. Technol.* **2** 226–245

[4] Son S., Park H. and Lee K. H. 2002 Automated laser scanning system for reverse engineering and inspection *Int. J. Mach. Tools Manuf.* **42** 889-897

[5] Boeckmans B., Zhang M., Welkenhuyzen F. and Kruth J.-P. 2014 Comparison of aspect ratio, accuracy and repeatability of a laser line scanning probe and a tactile probe *LMPMI* **11** 65-70

[6] Van Gestel N., Cuypers S., Bleys P. and Kruth J.-P. 2009 A performance evaluation test for laser line scanners on CMMs *Opt. Lasers Eng*. **47** 336-342

[7] Boeckmans B., Probst G., Zhang M., Dewulf W., Kruth J.-P. 2016 ISO 10360 verification tests applied to CMMs equipped with a laser line scanner *Proceedings SPIE Commercial + Scientific Sensing and Imaging* **9868**, art.nr. 9868-05

[8] Genta G., Minetola P. and Barbate G. 2016 Calibration procedure for a laser triangulation scanner with uncertainty evaluation *Opt. Lasers Eng*. **86** 11-19

[9] Tian Q., Yang Y., Zhang X. and Ge B. 2014 An experimental evaluation method for the performance of a laser line scanning system with multiple sensors *Opt. Lasers Eng.* **52** 241-249

[10] Wang Q., Zissler N. and Holden R. 2013 Evaluate error sources and uncertainty in large scale measurement systems *Robot. Comput. Integr. Manuf.* **29** 1-11

[11] Feng H.-Y., Liu Y. and Xi F. 2001 Analysis of digitizing errors of a laser scanning system *Prec. Eng*. **25** 185-191

[12] Bešić I., Van Gestel N., Kruth J.-P., Bleys P. and Hodolič J. 2011 Accuracy improvement of laser line scanning for feature measurements on CMM *Opt. Lasers Eng.* **49** 1274-1280

[13] Isa M. A. and Lazoglu I. 2017 Design and analysis of a 3D laser scanner *Meas*. **111** 122-133

[14] JCGM 101:2008, Evaluation of measurement data – Supplement 1 to the "Guide to the expression of uncertainty in measurement" – Propagation of distributions using a Monte Carlo method

[15] Boeckmans B., Tan Y., Welkenhuyzen F., Guo Y.S. Dewulf W. and Kruth J._P. 2015 Roughness offset differences between contact and non-contact measurements *Proc. Int. Conf. EUSPEN* **15** 189-190

[16] Boehler W., Vcent M. B. and Marbs A. 2003 Investigating laser scanner accuracy *Proc. CIPA XIXth Int. Sym.* **34**

[17] Wilhelm R.G., Hocken R. and Schwenke H. 2001 Task specific uncertainty in coordinate measurement *CIRP Annals* **50** 553-563